

PDF hosted at the Radboud Repository of the Radboud University Nijmegen

The following full text is a publisher's version.

For additional information about this publication click this link.

<http://hdl.handle.net/2066/91983>

Please be advised that this information was generated on 2019-03-25 and may be subject to change.



LOFAR: Detecting Cosmic Rays with a Radio Telescope

A. CORSTANJE¹, M. VAN DEN AKKER¹, L. BÄHREN^{1,4}, H. FALCKE^{1,2}, J. R. HÖRANDEL¹, A. HORNEFFER^{1,5}, C. W. JAMES¹, J. L. KELLEY¹, M. MEVIUS³, P. SCHELLART¹, O. SCHOLTEN³, S. THOUDAM¹, S. TER VEEN¹

¹*Department of Astrophysics, IMAPP, Radboud University Nijmegen, 6500GL Nijmegen, The Netherlands*

²*Netherlands Institute for Radio Astronomy (ASTRON), 7990AA Dwingeloo, The Netherlands*

³*Kernfysisch Versneller Instituut, 9747AA Groningen, The Netherlands*

⁴*now at: Anton Pannekoek Astronomical Institute, University of Amsterdam, 1090 GE Amsterdam, The Netherlands*

⁵*now at: Max-Planck-Institut für Radioastronomie, 53121 Bonn, Germany*

a.corstanje@astro.ru.nl

Abstract: LOFAR (the Low Frequency Array), a distributed digital radio telescope with stations in the Netherlands, Germany, France, Sweden, and the United Kingdom, is designed to enable full-sky monitoring of transient radio sources. These capabilities are ideal for the detection of broadband radio pulses generated in cosmic ray air showers. The core of LOFAR consists of 24 stations within 4 square kilometers, and each station contains 96 low-band antennas and 48 high-band antennas. This dense instrumentation will allow detailed studies of the lateral distribution of the radio signal in a frequency range of 10-250 MHz. Such studies are key to understanding the various radio emission mechanisms within the air shower, as well as for determining the potential of the radio technique for primary particle identification. We present the status of the LOFAR cosmic ray program, including the station design and hardware, the triggering and filtering scheme, and the status of searches for cosmic-ray-induced radio pulses.

Keywords: radio, air shower, LOFAR, LORA

1 Introduction

Radio emission from cosmic ray air showers was discovered in 1965 by Jelley and collaborators [1]. Advances in high-speed digital electronics have expanded the options for filtering, triggering, and recording the radio signal and have led to renewed interest in the technique. This window on high-energy cosmic rays has a duty cycle of nearly 100% and can in principle, like the air fluorescence technique, provide information on shower development in the atmosphere.

The LOFAR Prototype Station (LOPES) successfully detected the coherent radio pulses from air showers with energies from 5×10^{16} to 5×10^{17} eV in a frequency range of 43-73 MHz. LOPES verified the primary nature of the emission from the air shower: the interaction of shower electrons and positrons with the Earth's magnetic field [3]. Since then, significant progress has also been made in the theoretical understanding of the radio signals [4], with current work focused on sub-dominant emission mechanisms, such as charge excess and Cherenkov contributions.

LOFAR, the Low Frequency Array, is a digital radio telescope with a dense core of antennas capable of detecting air shower pulses and recording the signal polarization and

lateral distribution with unprecedented accuracy. Understanding and modeling all details of the radio emission will allow a full demonstration of the potential for determining fundamental cosmic ray properties from the radio signal, such as primary particle type [5, 6].

2 LOFAR

LOFAR is a digital aperture-synthesis radio telescope consisting of at least 48 stations. 24 core stations are concentrated within a 4-km² area near Exloo in the Netherlands, 16 remote stations are distributed up to 65 km from the core throughout the northern Netherlands, and 8 international stations are spread between England, France, Germany, and Sweden. Unlike typical ground-based cosmic ray detectors, the density of LOFAR stations from the core falls off smoothly, from six stations in the "superterp" (the 360 m diameter island at the center of the LOFAR core; see Fig. 1), to effectively isolated remote and international stations.

Each station consists of either one or two high-band antenna (HBA) fields, covering the frequency range 110-250 MHz, and a low-band antenna (LBA) field, covering the 10-80 MHz range. The HBA fields consist of between 24



Figure 1: Photograph of the LOFAR superterp – pictured are twelve HBA core fields (grey squares) and six LBA fields (barely visible).



Figure 2: Photograph of a LOFAR droop-dipole low-band antenna (LBA).

and 96 tiles of 4×4 bowtie antennas, while the LBA fields each consist of 96 dual-polarization droop-dipole antennas (see Fig. 2), 48 of which can be used simultaneously (on the core and remote stations). The LOFAR Cosmic Rays Key Science Project aims to use the LBAs to detect atmospheric cosmic ray air showers in parallel with standard LOFAR operations.

As a fully digital telescope, LOFAR uses digital signal processing to focus the signals from individual station elements, in contrast to traditional telescopes which use geometrical optics (curved mirrors). Signals from individual elements (LBA dipoles or HBA tiles) are digitized at 200 MHz^1 with 12-bit precision. The digitized signals are divided into 512 frequency sub-bands, up to 240 of which can be added together with appropriate phase offsets to form up to eight station beams viewing between ~ 2 and ~ 1700 square degrees each, depending on the frequency selection and antenna configuration [2]. These beams are then sent to the LOFAR central processing hub in Groningen for cross-correlation (imaging) or further beam-forming (e.g. for pulsar searches).

Station Type	Number	LBA	HBA
Core	24	96*	2x24
Remote	16	96*	48
International	8	96	96

Table 1: Summary of the LOFAR station types. *Only 48 can be used simultaneously.

In parallel to station beam-forming, the digitized time-domain signals from each station element can also be analyzed with real-time logic and/or copied to LOFAR’s Transient Buffer Boards (TBBs), circular RAM buffers holding up to 1.3 seconds of data from each station element. Data from the TBBs can be accessed and returned for processing without interfering with other observation modes.

The LOFAR Cosmic Rays Key Science Project is using this parallel capability to search for atmospheric cosmic ray events. The LBAs individually provide all-sky coverage, and their sensitivity peaks in the 30-80 MHz range where the maximum radio signal from extensive air showers (EAS) has been observed [3]. The LOFAR “VHECR” (very-high-energy cosmic ray) mode utilizes the LBAs for a real-time search for EAS signatures, and its implementation and operation is the subject of this contribution. The “HECR” (high-energy cosmic ray) mode, which trades sky coverage for increased sensitivity by using station beams to search for EAS, will be developed in the near future, while the “UHEP” (ultra-high-energy particles) mode, by which beams from all stations target the Moon to detect particle interactions in the Lunar regolith, is the subject of another contribution [7].

2.1 Triggering and Data Acquisition

In VHECR mode, LOFAR can trigger on cosmic rays in two ways: directly on the radio air shower signal, or via an external trigger (e.g. from a particle detector array). Radio triggering is performed in two stages, and the time-series signal around a pulse is stored for all channels once the highest-level trigger is satisfied.

Our first-level trigger is based upon that developed for the LOPES experiment [9]. Pulses are detected in real-time, by processing the digitized radio signal of each polarization channel in an FPGA (field-programmable gate array). The FPGA performs a threshold search on the absolute values of the voltage ADC samples using the criterion

$$|x_i| > k \mu_i, \quad (1)$$

where μ_i is a running average over the previous 4096 absolute values, and k is an integer threshold factor, typically set between 6 to 8. If we assume the background signal to be Gaussian-distributed with standard deviation σ , the mean absolute value is related to σ as

$$\mu = \sqrt{\frac{2}{\pi}} \sigma \simeq 0.8 \sigma, \quad (2)$$

and thus the threshold is typically a factor of 5 to 6 above the time-varying noise level. When this threshold is crossed, a message is passed to the station’s control PC, where the second-level trigger operates. The message contains a number of parameters characterizing the pulse, including trigger time, pulse height, pulse width, and noise levels before and after the pulse.

1. A 160 MHz mode is also possible, but is used less frequently.

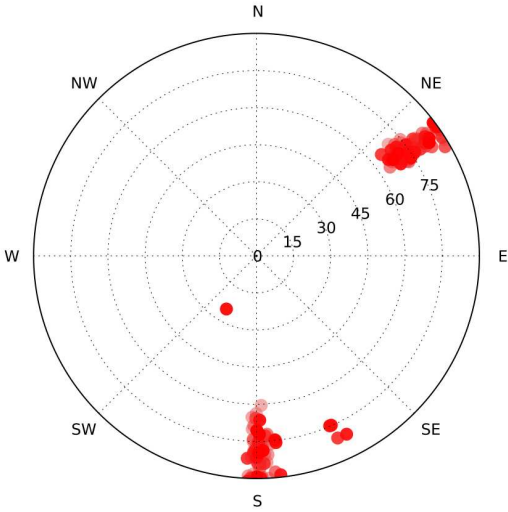


Figure 3: Example of pulse arrival directions as calculated from trigger arrival times. The center represents the zenith; the outer edge corresponds to the horizon. Shown are two fixed interference sources and one pulse from a high elevation that would pass the trigger conditions.

The second-level trigger searches for coincidences between single-channel triggers. Typically, we require 16 to 32 out of 96 channels to trigger within a $1 \mu\text{s}$ time window. For these events, we perform a real-time direction estimate based on the first-level trigger times and the antenna positions, sample results of which are plotted in Fig. 3. Although the uncertainty in time of the trigger messages is about 2 to 3 samples (i.e. 10-15 ns), the estimated source direction is accurate enough to distinguish between sources from the sky and interference sources on the horizon. The coincidence event rate is dominated by a few fixed radio-frequency interference (RFI) sources — most commonly electric fences around nearby farm fields — that emit pulsed radiation semi-continuously, roughly every second. Therefore, the second-level trigger also uses this preliminary reconstruction to exclude triggers coming from within 30° of the horizon.

When a pulse passes all second-level trigger criteria, the buffered time-series data for 0.5 to 1 ms around the pulse are sent to an archive for offline analysis. The relatively large size of this data window allows offline spectral cleaning of narrow-band radio transmitters from the signal with a frequency resolution of 1 to 2 kHz.

In addition to the radio-triggering mode, LOFAR can also be triggered by an external particle detector array. LORA (the LOFAR Radboud Air Shower Array) is an array of 20 plastic scintillator detectors arranged in 5 stations within the LOFAR superterp [8]. Upon detection of an air shower by LORA, a trigger can be sent to LOFAR to store the radio signal from all dipoles for further analysis. This can be used to provide an unambiguous cross-check that a radio signal is from an EAS, and can also be used to reduce the detection energy threshold, as described in Sec. 2.3.

2.2 Data Analysis

We process the second-level trigger data using an automated pipeline structure, the first objective being to discriminate cosmic ray (CR) events from other pulses. The following steps are performed:

1. data validation, e.g. elimination of pulse trains or other noise;
2. matching of the event data with coincident triggers from particle detectors and/or other LOFAR stations;
3. spectral cleaning, i.e. removal of narrow-band radio transmitters from the spectrum; and
4. reconstruction of the source position (direction and distance).

To locate the source, we calculate the “beam-formed” time-series for a set of directions and distances. Assuming a point source at a given position, we correct for the relative time delays at each antenna, using a spherical-wavefront approximation. The sum of delay-corrected signals from all antennas gives the beam-formed signal (see Fig. 4). As the true source position can be identified as the one yielding the maximum pulse power in the beam-formed signal, the best-fit direction can be efficiently found using a downhill-simplex algorithm, using the second-level trigger’s direction estimate as a starting point for the search. The results of the pipeline can then be used to determine key air shower event parameters such as energy and position of shower maximum.

2.3 Energy Threshold and Estimated Event Rate

The detection energy threshold of the VHECR mode is determined at minimum by the first-level trigger on an individual LBA dipole. An event with signal exactly equal to the threshold will trigger on average half of the dipoles at station level (thus passing the multi-channel trigger requirement), and will not be rejected as RFI unless it is a highly-inclined event with zenith angle larger than 60° . Thus, the second-level trigger restricts the sky to π sr for real events.

The noise background against which cosmic ray signals must be detected is dominated by the Galactic background emission, with effective temperature at wavelength λ given by $T_{\text{sky}} = 60 \pm 20(\lambda/\text{m})^{2.55}$ K [2]. The sky temperature is in turn defined using the measured flux $I(\nu)$ via the Rayleigh-Jeans Law of $I(\nu) = 2k_B T_{\text{sky}} \lambda^{-2}$, where k_B is Boltzmann’s constant. The (sparse) outer LBAs have an effective area A_{eff} that increases with wavelength: $A_{\text{eff}} \approx \lambda^2/3$. As there is strong RFI below 30 MHz, we use a filter which limits our bandpass to approximately 30-80 MHz; after filtering, RFI typically contributes an additional 25% to our system noise. Assuming constant effective area over the observed solid angle Ω_{sky} and accounting for RFI, the noise power P_n received in a single polar-

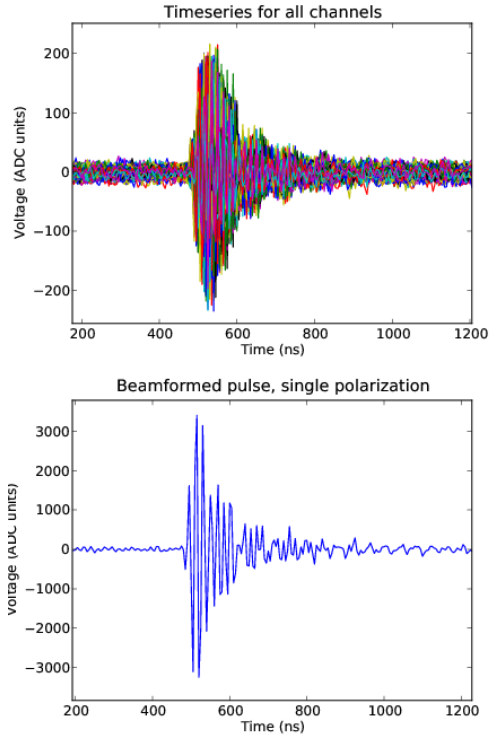


Figure 4: Top: time-series radio signal for all channels individually (superimposed). Bottom: the beam-formed signal, in the same voltage units. Note the much larger pulse height as well as a larger signal-to-noise ratio in the beam-formed signal.

ization channel can be calculated by integrating over frequency ν :

$$P_n = 1.25 \Omega_{\text{sky}} \int \frac{k_B T_{\text{sky}}(\nu)}{\lambda^2} A_{\text{eff}}(\nu) f(\nu) d\nu \quad (3)$$

where $f(\nu)$ is the power response of the filter. The radio signal V_{eas} of an extensive air shower is coherent and must be calculated in the voltage domain from its intrinsic field strength $S(\nu)$ and angle θ_p of the receiver to the polarization vector:

$$V_{\text{eas}} = \cos \theta_p \int S(\nu) \sqrt{f(\nu) A_{\text{eff}}(\nu)} d\nu. \quad (4)$$

This must sufficiently exceed the RMS noise voltage $V_{\text{rms}}^2 = P_n Z_0$ in order to result in a trigger. Simulations of the expected signal $S(\nu)$ indicate an increased strength at lower frequencies [4]; however, we use an empirical frequency-independent parameterization based on LOPES measurements [10].

Using a trigger threshold of $|V_{\text{eas}}| > 5|V_{\text{rms}}|$, we find a minimum energy threshold of $\sim 5 \times 10^{16}$ eV. However, the strength of the geomagnetic emission mechanism is strongly dependent on the angle between the shower axis and the Earth's magnetic field, and a typical shower geometry results in a threshold closer to 10^{17} eV. Taking the station effective area to be equal to that of a circle with radius given by the characteristic signal fall-off length of ~ 200 m [10], the total expected event rate for all 40 core and remote

stations will be of the order of 1/hr. The coincidence rate of the superterp stations with the LORA particle detector is estimated to be of order 1/day.

For LORA-triggered events (where the arrival direction is given by the particle detectors), the radio threshold is given instead by the beam-formed data from all 48 antennas. Thus the threshold for LORA events will be lower than radio-only mode by a factor of between $\sqrt{48}$ and $\sqrt{96}$, depending on the relative strengths of the signal in each of the polarization channels (2 per antenna). Therefore we expect a threshold of $\sim 10^{16}$ eV over the central region covered by LORA, and a corresponding event rate of order 2/hr.

2.4 Current Status and Outlook

As of May 2011, the first and second-level triggers are operational, as well as the offline analysis pipeline described in the previous section. Directional reconstruction of pulses with an angular resolution of 1 to 2 degrees is possible using single-station data. Distance estimates to the shower core will be improved by considering multiple LOFAR stations for the same event (i.e. longer baselines). Reconstruction methods using more sophisticated wavefront shapes are also under development.

Optimization of the radio trigger algorithms will allow a reduction of deadtime as well as the veto of RFI sources from above the horizon, such as those from airplanes. The external trigger from the LORA particle array is being finalized and will allow an important cross-check of the radio trigger as well as unambiguous identification of radio signals from air showers. This will in turn lead to the most densely instrumented measurements of air shower radio emission to date.

References

- [1] J. V. Jelley *et al.*, *Nature*, 1965, **205**:327.
- [2] The LOFAR collaboration, *LOFAR: The Low Frequency Array* (in preparation); www.astron.nl
- [3] H. Falcke *et al.*, *Nature*, 2005, **435**:313.
- [4] T. Huege *et al.*, *Nucl. Instr. Meth. A*, in press; arXiv:1009.0346.
- [5] K. D. de Vries *et al.*, *Astropart. Phys.*, 2010, **34**:267-273.
- [6] T. Huege, R. Ulrich, and R. Engel, *Astropart. Phys.*, 2008, **30**:96-104.
- [7] S. ter Veen *et al.*, 2011, contribution ID 1042 (these proceedings).
- [8] J. R. Hörandel *et al.*, 2011, contribution ID 1017 (these proceedings).
- [9] A. Horneffer *et al.*, *Nucl. Instrum. Meth. Suppl.*, 2009, A604:20-23.
- [10] A. Horneffer *et al.*, *Primary Particle Energy Calibration of the EAS Radio Pulse Height*, Proceedings of the 30th ICRC, Mérida, Mexico (2007).